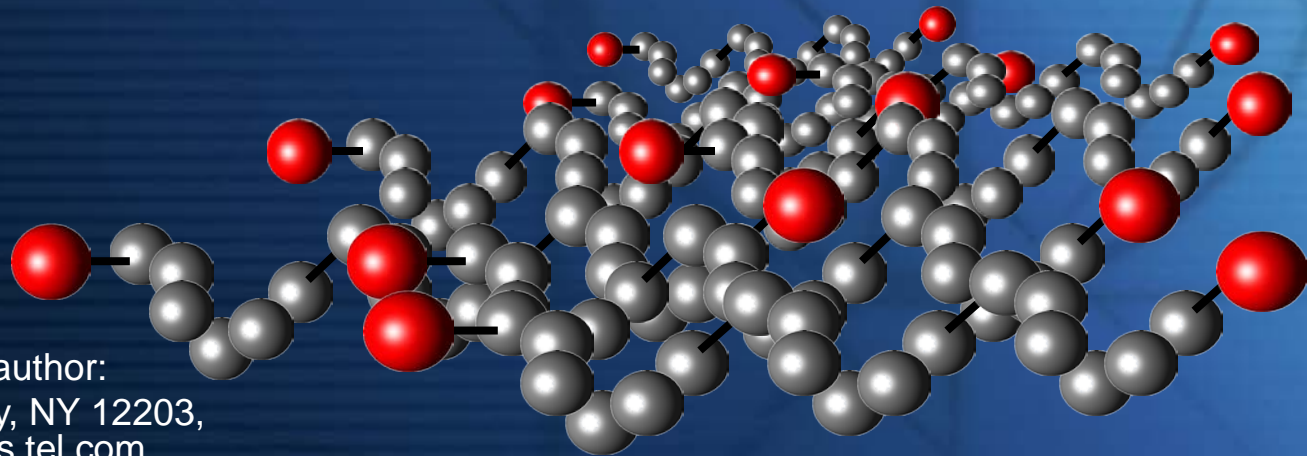




Model of a Filament Assisted CVD reactor

Jozef Brcka*

TEL US Holdings, Inc., Technology Development Center



*Corresponding author:

255 Fuller Rd., Albany, NY 12203,

jozef.brcka@us.tel.com

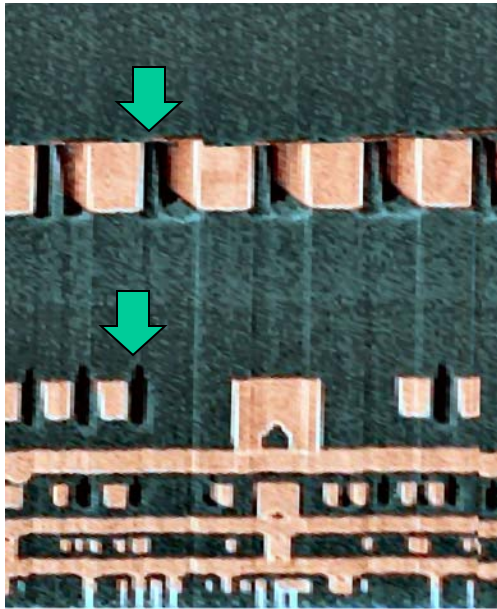


TOKYO ELECTRON

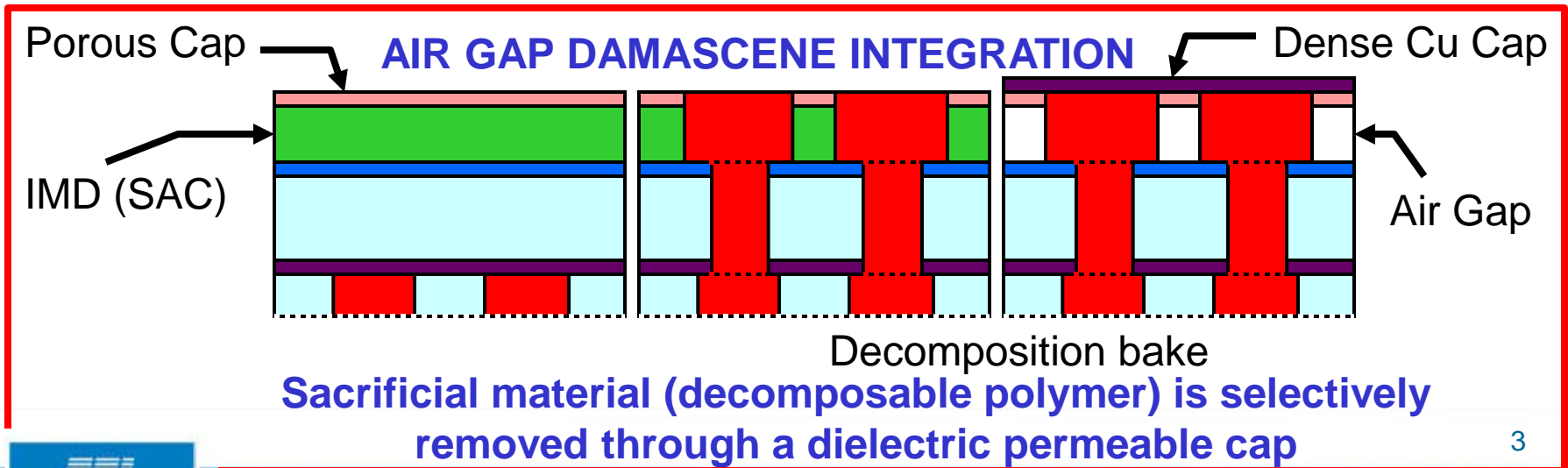
FACVD method ...

- Deposition of polymer films – with original functionality without introduction of a damage
- FACVD , iCVD - dry process and non-plasma environment
- Suitable precursors are thermally activated into radical components which participate directly on the film growth or are initiating those processes
- Substrate at room temperature
- Thermal activation by very moderate temperatures ~ 200 °C - several hundreds
- Applications extending from semiconductor technology into nanotechnology

Motivation ...

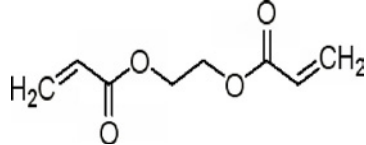
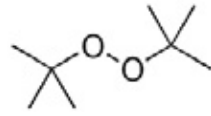
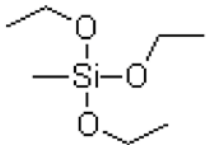


- ❑ Air-gap applications in semiconductor devices:
The basic principle consists of dielectric material removal (from in-between the metal lines)
- ❑ Other applications: organic devices, bio-passivation, 3D interconnect, and energy
 - ✓ Transfer specific process from laboratory experimentation towards semiconductor processing tool
 - ✓ Match and optimize chemistry and process - enhanced flexibility of a process development

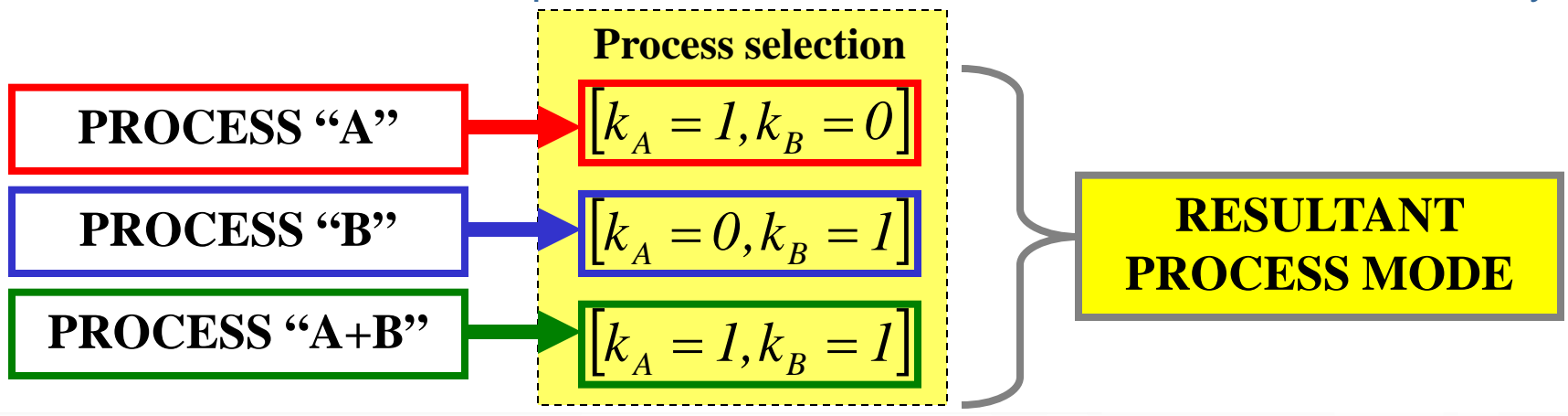


Precursors and chemistry

- ❑ Precursors w low decomposition T
- ❑ Compatibility with semiconductor processing
- ❑ More complex mixture and chemistry for an increased adhesion, film properties, ...

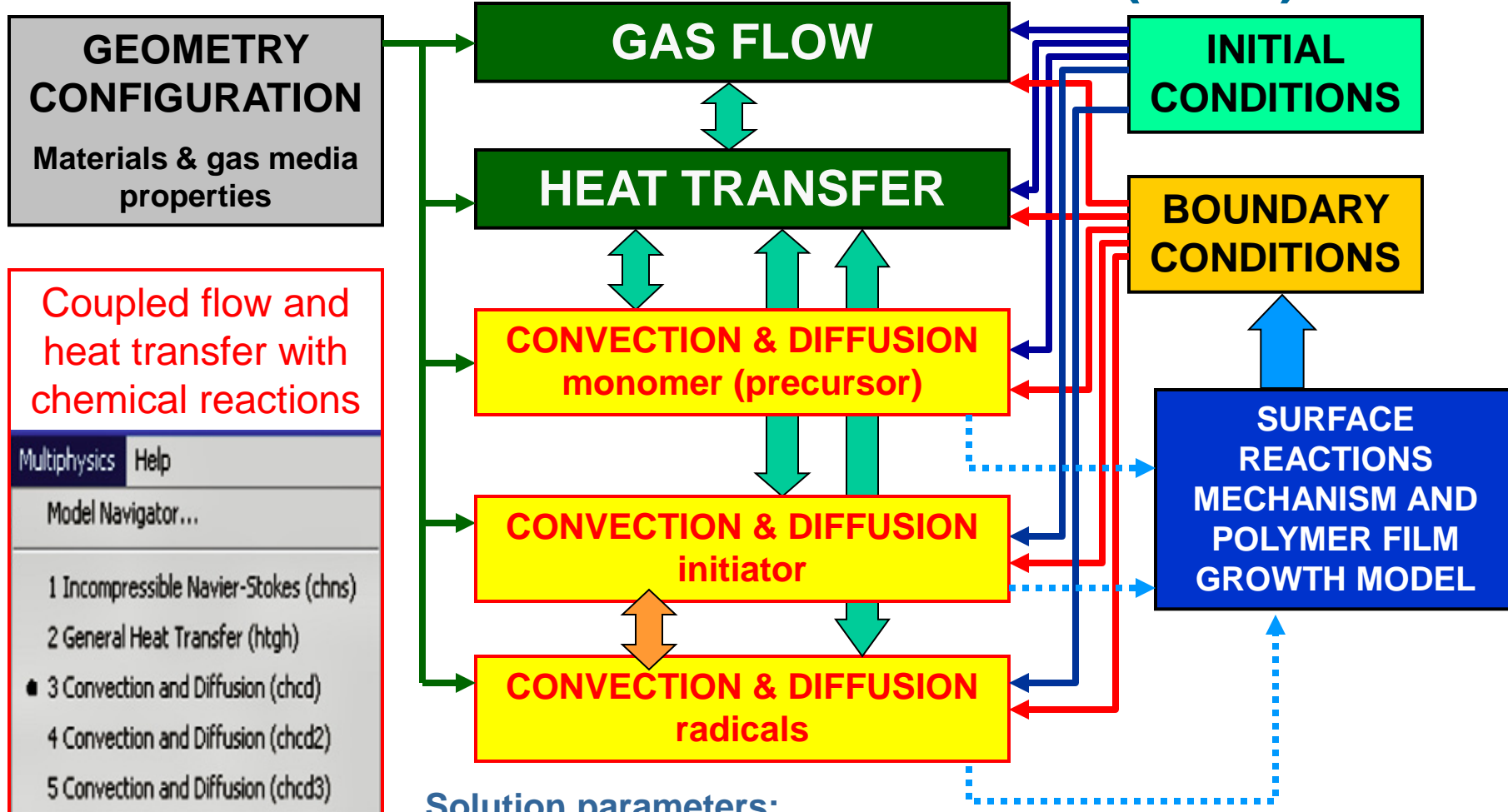
EGDA ETHYLENE GLYCOL DIACRYLATE	TBPO TERT-BUTYL PEROXIDE	MTEOS METHYLTRIEHOXY- SILANE
$C_8H_{10}O_4$	$C_8H_{18}O_2$	$C_7H_{18}O_3Si$
		

“**LOGIC SWITCHES**” implemented to use same model for different chemistry



FACVD model

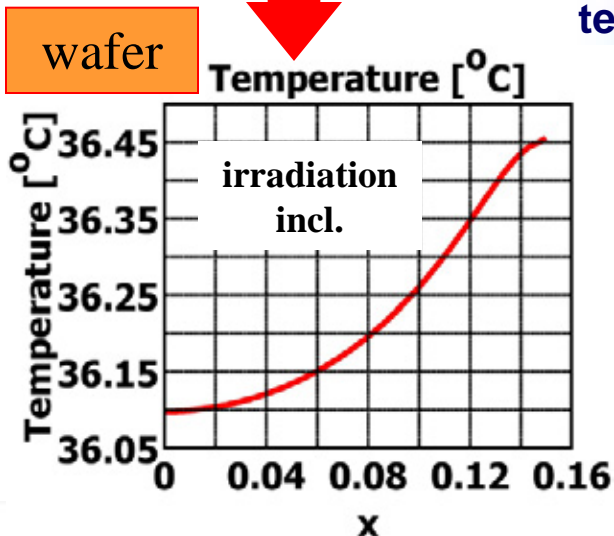
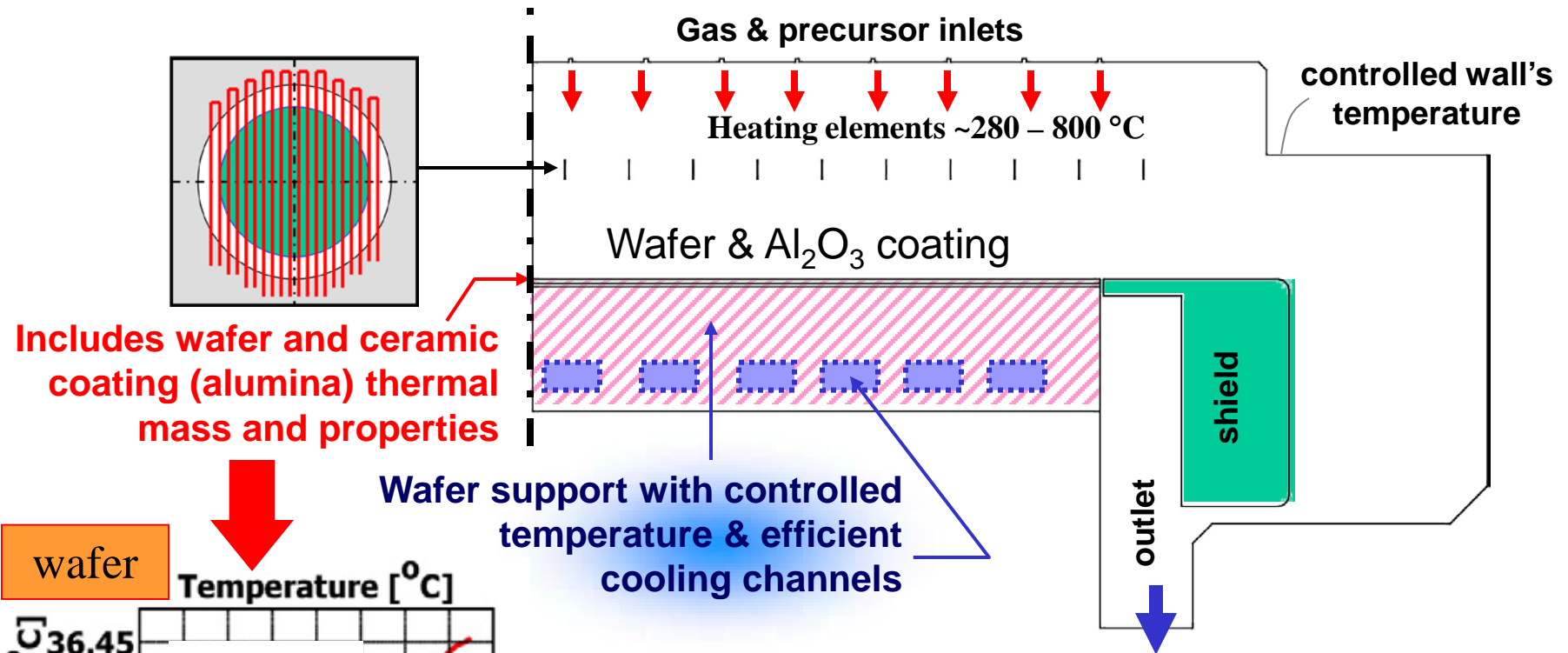
Comsol-based scheme (v.3.5)



Solution parameters:
Stationary Analysis types
Direct (PARDISO) solver



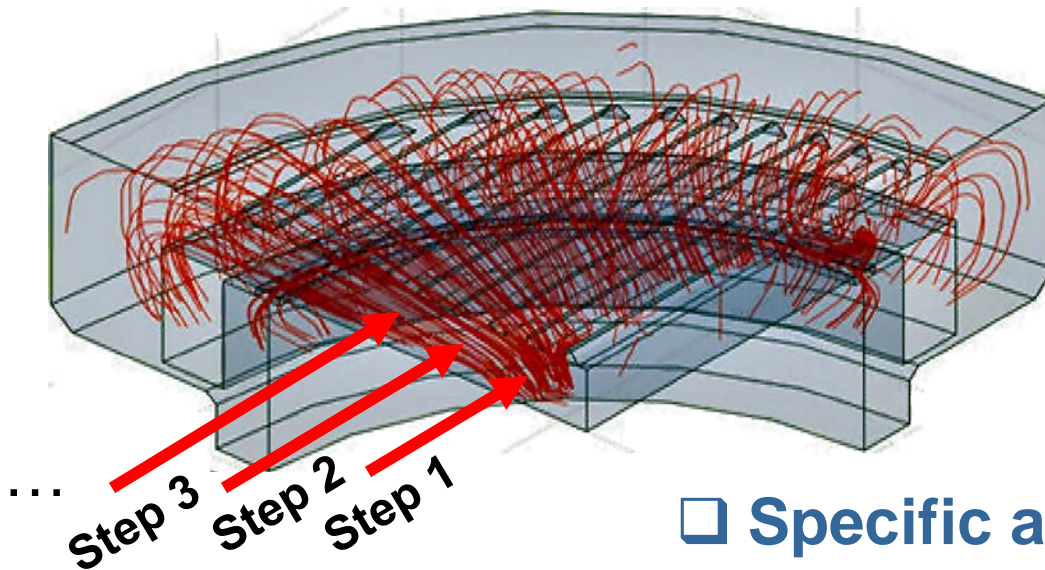
Model geometry & features



2D model in Cartesian coordinate system

- Detailed inlets geometry
- Radiation from heater elements to wafer (analytical approach - it consider a heater's element geometry)
- Variable coating thickness under wafer

3D model - gas flow computation



To achieve converging solution in full geometry – ongoing recurrent simulations were performed

page file usage up to 18.5 GB

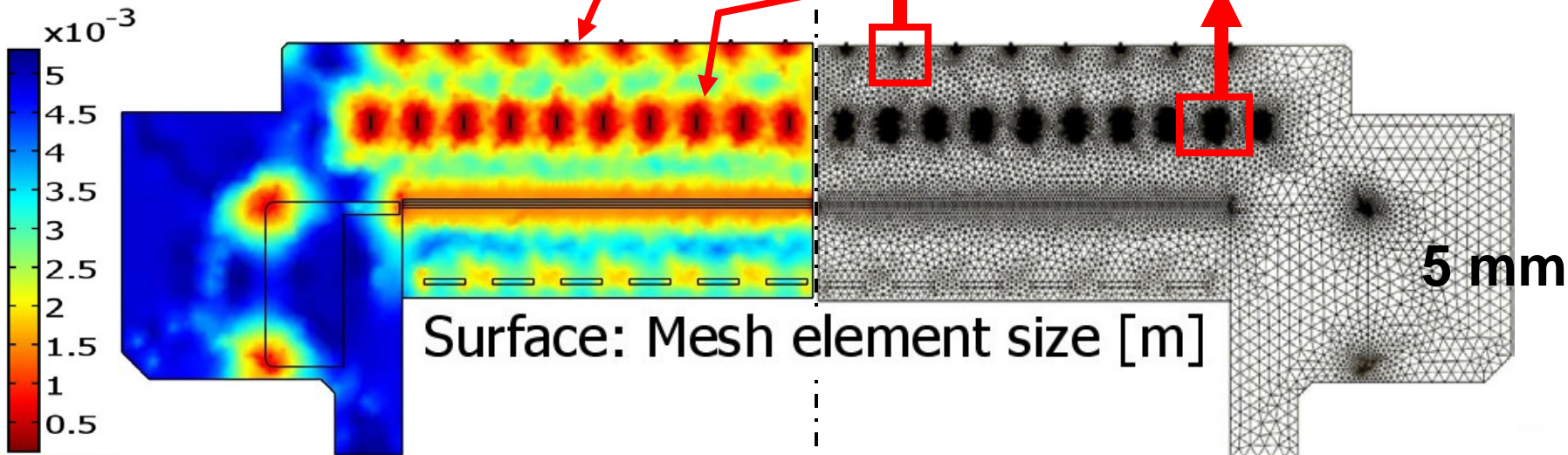
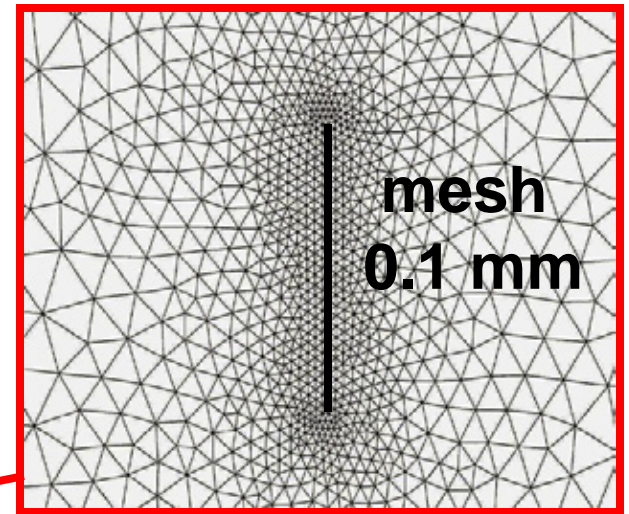
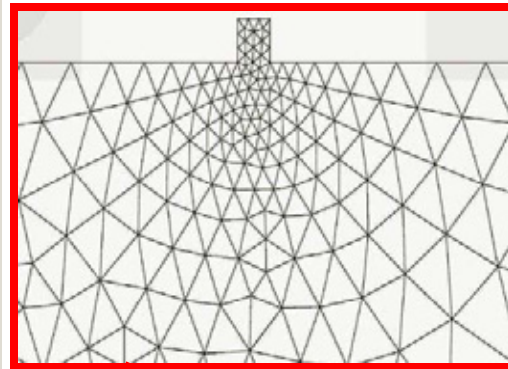
dual duo-core CPU usage at 100 %

- ❑ Specific asymmetry due to multi-linear heater and quasi-axial symmetry of the flow
- ❑ Approach for 3D computations to validate 2D cartesian model
- ❑ ⇒ Significant time resources could be saved

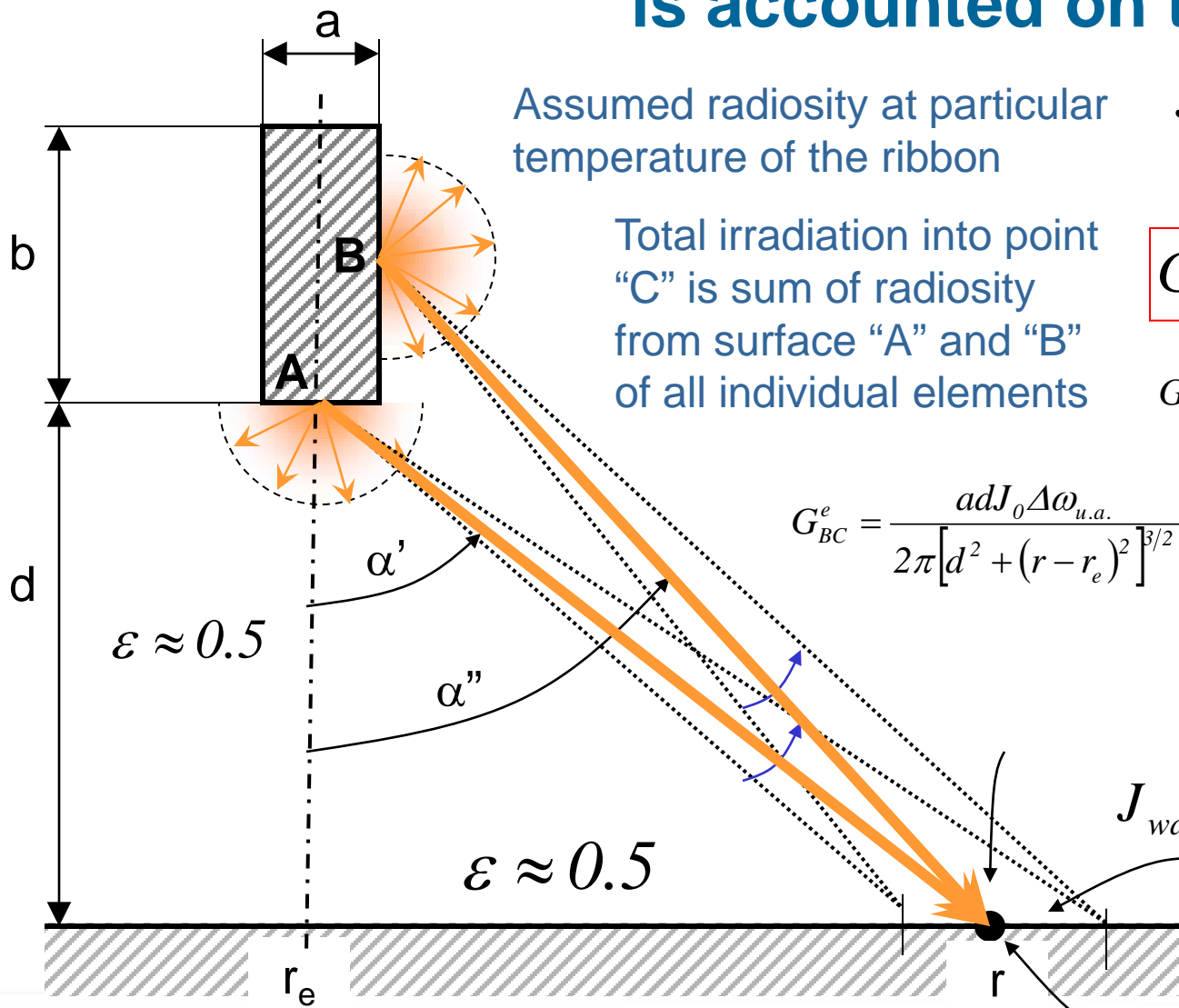
Meshing properties

Mesh Statistics			
Global	Subdomain	Boundary	Point
Extended mesh:			
Number of degrees of freedom:		365681	
Base mesh:			
Number of mesh points:		16284	
Number of elements:		32151	
Triangular:		32151	
Quadrilateral:		0	
Number of boundary elements:		1616	
Number of vertex elements:		126	
Minimum element quality:		0.7892	
Element area ratio:		3.84E-4	

- Mesh size
~0.1 mm – 5 mm



Radiant power from heater is accounted on the wafer



Assumed radiosity at particular temperature of the ribbon

Total irradiation into point "C" is sum of radiosity from surface "A" and "B" of all individual elements

$$J_0 \left[Wm^{-2} \right] = \epsilon \sigma T_{heater}^4$$

$\epsilon \approx 0.03 - 0.75$

$$G_C^e \approx G_{AC}^e + G_{BC}^e$$

$$G_{AC}^e = \frac{adJ_0\Delta\omega_{u.a.}}{2\pi[d^2 + (r-r_e)^2]^{3/2}}$$

$$G_{BC}^e = \frac{adJ_0\Delta\omega_{u.a.}}{2\pi[d^2 + (r-r_e)^2]^{3/2}} \times \frac{b(d+b/2)}{ad \left[\frac{(d+b/2)^2 + (r-r_e)^2}{d^2 + (r-r_e)^2} \right]^{3/2}}$$

$$\Delta\omega_{u.a.} \sim \left[1 + (r-r_e)^2/d^2 \right]^{-1/2}$$

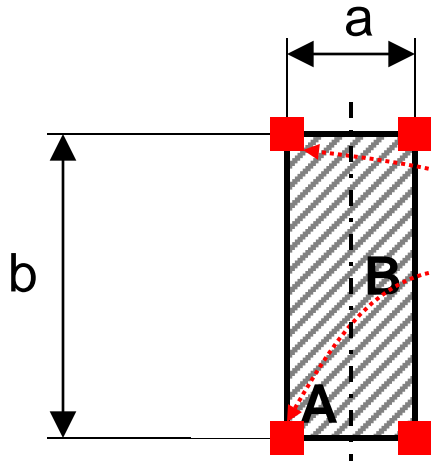
$$J_{wafer} = \epsilon \sigma (T_{heater}^4 - T_{wafer}^4)$$

unit area irradiation into the point "C" at the wafer surface



Heater averaged temperature

Point Integration Variables



T_{heater}

Point Integration Variables

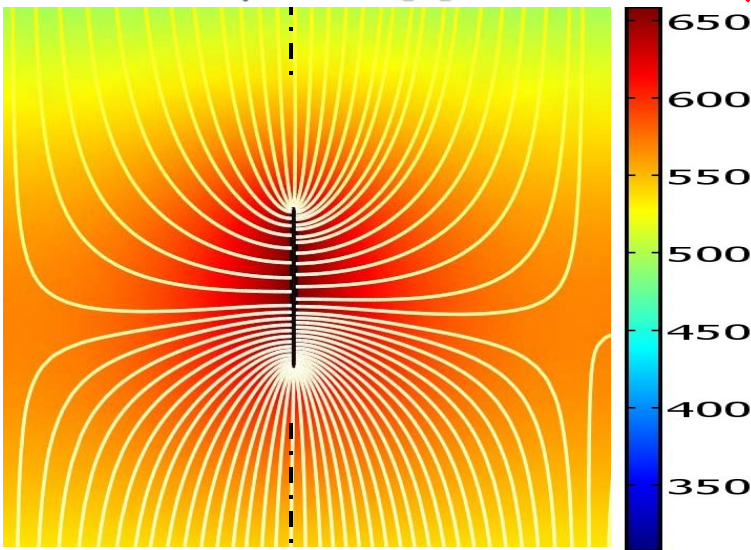
Source Destination

Point selection

Name	Expression	Global destination
TRR01	T/4	<input checked="" type="checkbox"/>
TRR02		<input checked="" type="checkbox"/>
TRR03		<input checked="" type="checkbox"/>
TRR04		<input checked="" type="checkbox"/>
TRR05		<input checked="" type="checkbox"/>
TRR06		<input checked="" type="checkbox"/>
TRR07		<input checked="" type="checkbox"/>
TRR08		<input checked="" type="checkbox"/>
TRR09		<input checked="" type="checkbox"/>
TRR10		<input checked="" type="checkbox"/>
		<input checked="" type="checkbox"/>
		<input checked="" type="checkbox"/>

Select by group

Surface: Temperature [K]

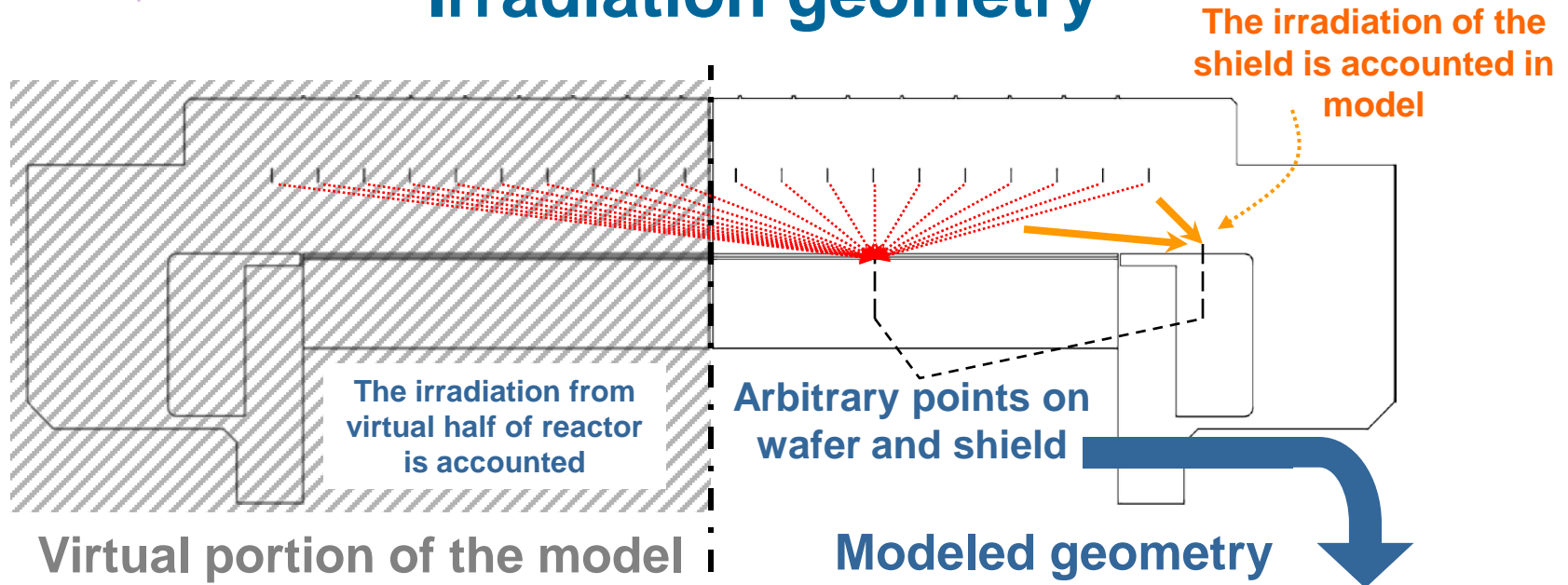


Streamline: Conductive heat flux

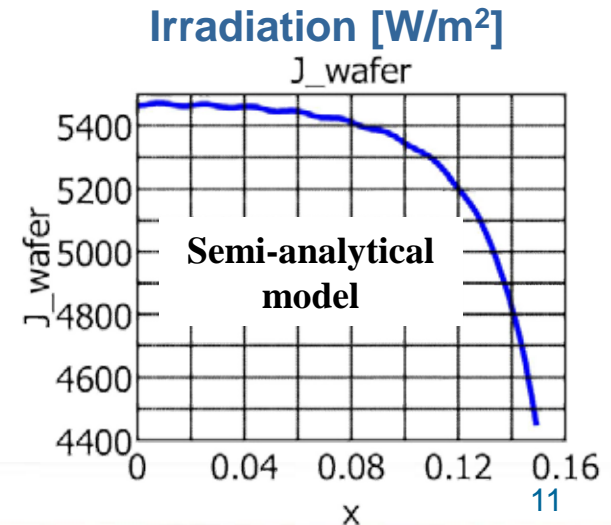
Detail of the single heating element



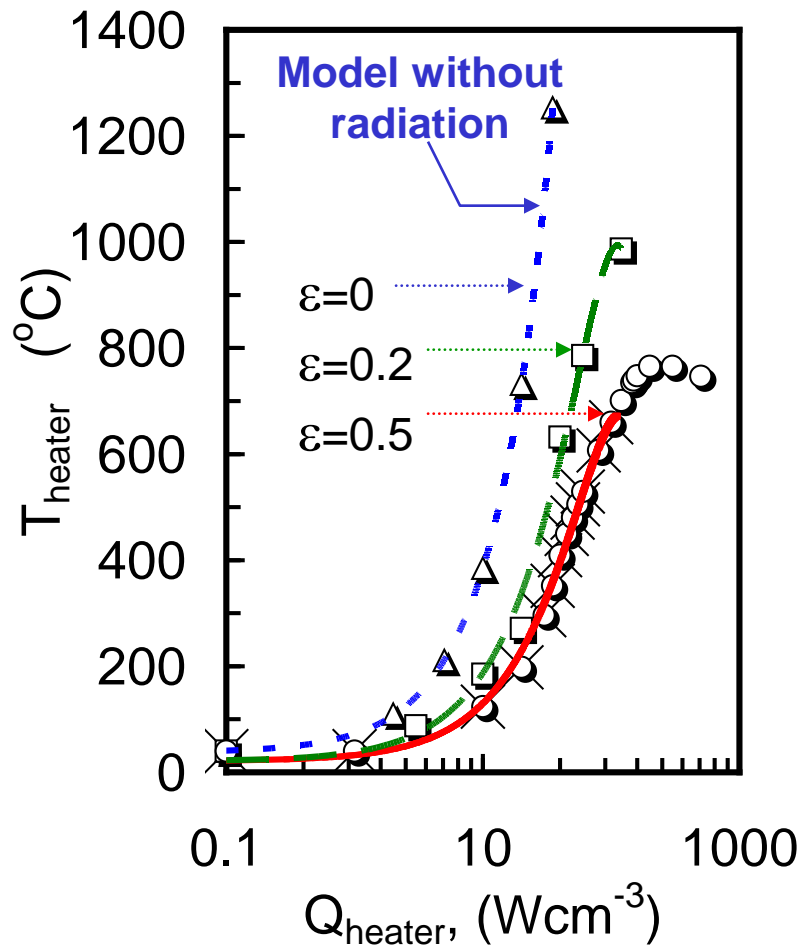
Irradiation geometry



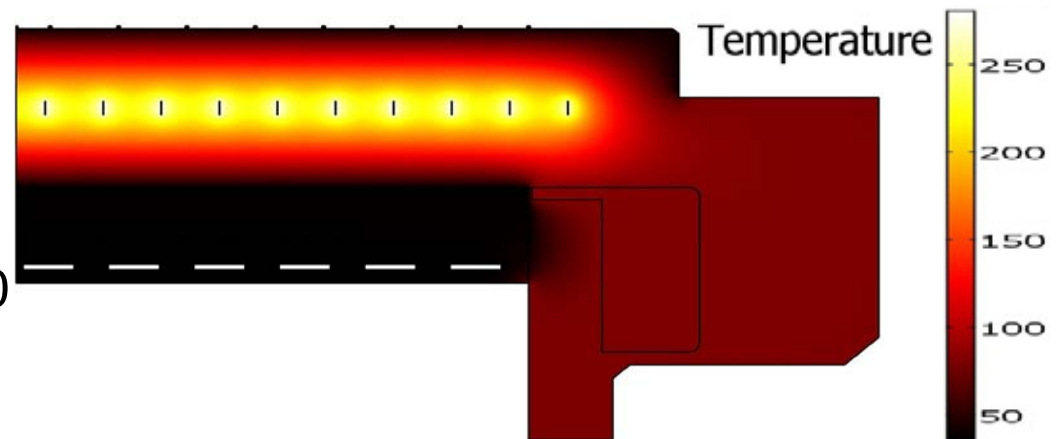
- radiation - loss at elements and increased T at wafer
- radiosity is uniform from planar heating assembly (planar source, no edge effect)
- No integration in normal direction to geometry
- Reflection on the wafer and ribbons is set to = 0
- Formally, the alumina coating is assumed to be 1 micron thick (actual geometry is 1 mm thick)



Impact of NiCr emissivity

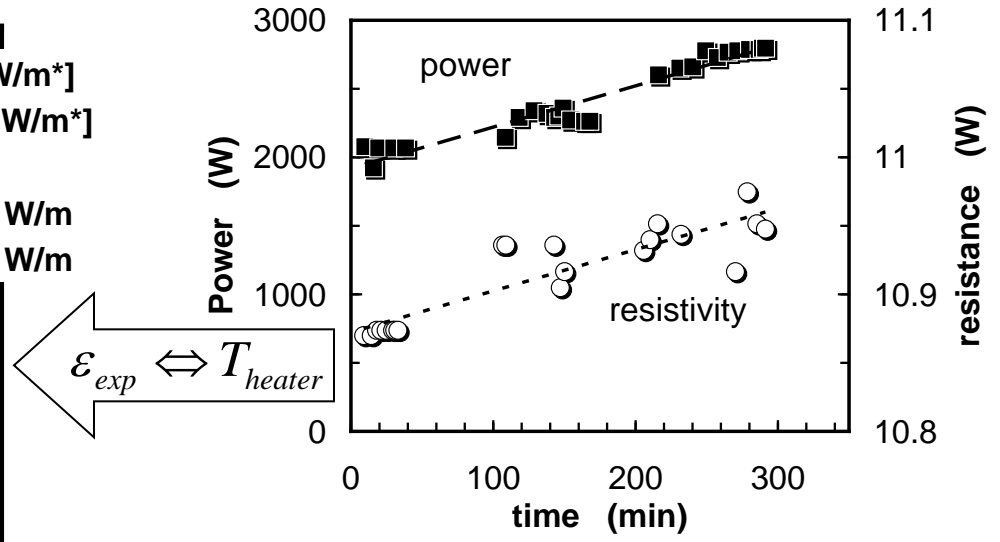
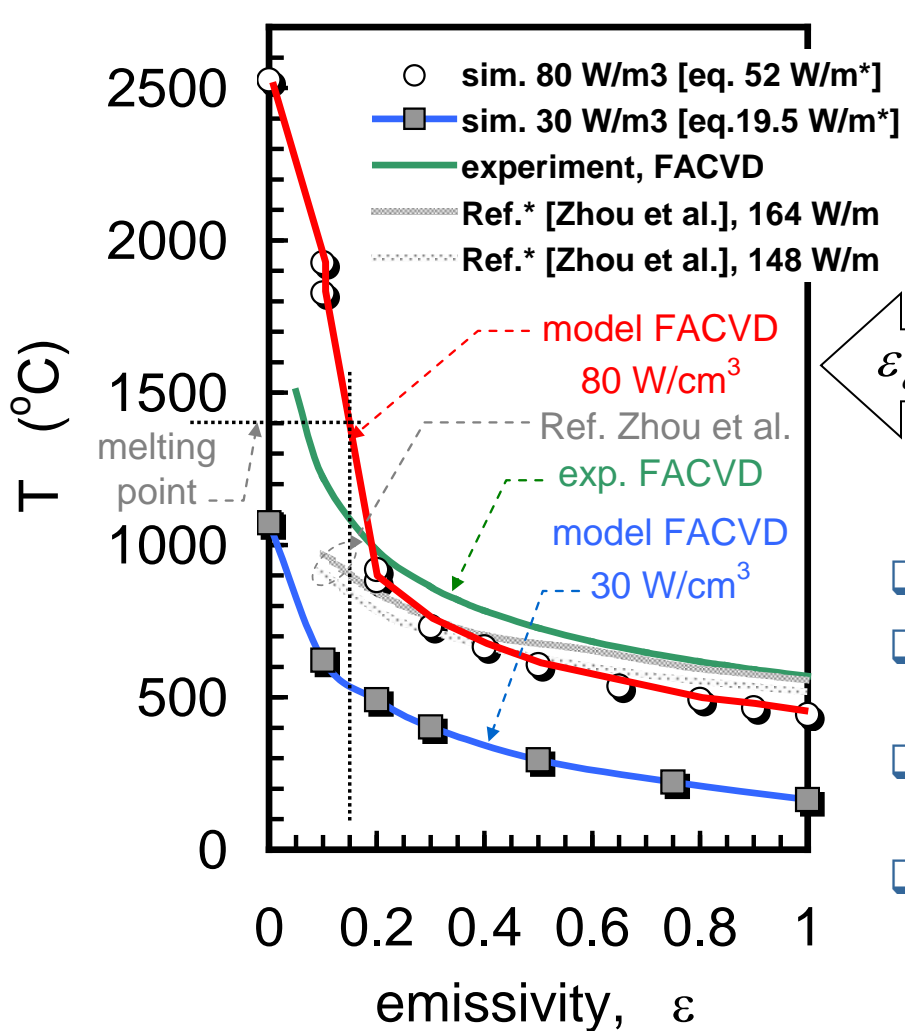


- Clean surface emissivity from 0.2 to 0.3 – aging over time
- Model provides
 - ✓ Identification of the operation window for particular HW geometry
 - ✓ Process sensitivity to heater aging
 - ✓ To address process control issues



Ref.: Y. S. Touloukian and D. P. DeWitt, *Thermal Radiative Properties - Metallic Elements and Alloys, Thermophysical Properties of Matter* (IFI/Plenum, New York, 1970).

NiCr emissivity performance

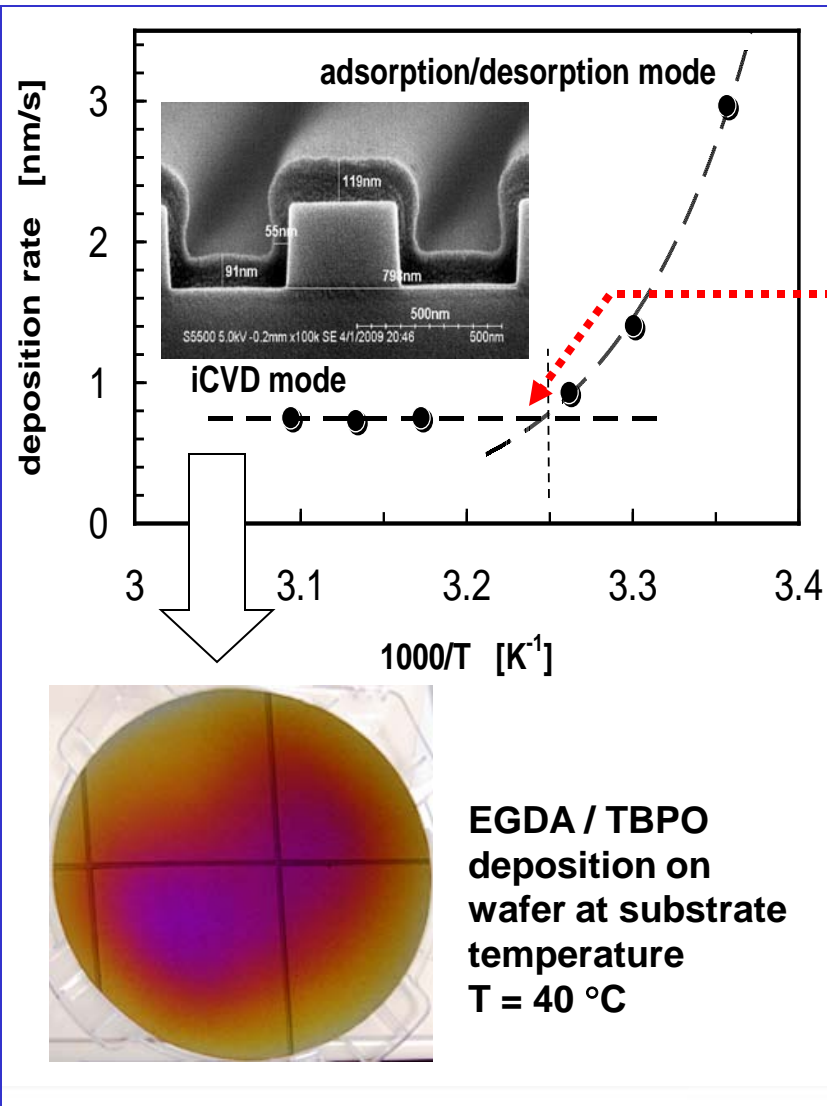


- Model correlates with published data
- Good validation with measurements in our FACVD reactor
- When $\epsilon < 0.2$ increased sensitivity of model \Rightarrow consideration of 3D
- “clean” NiCr ($\epsilon \sim 0.4$) to “heavily oxidized” surface ($\epsilon \sim 0.85$) generates temperature change – important for process control

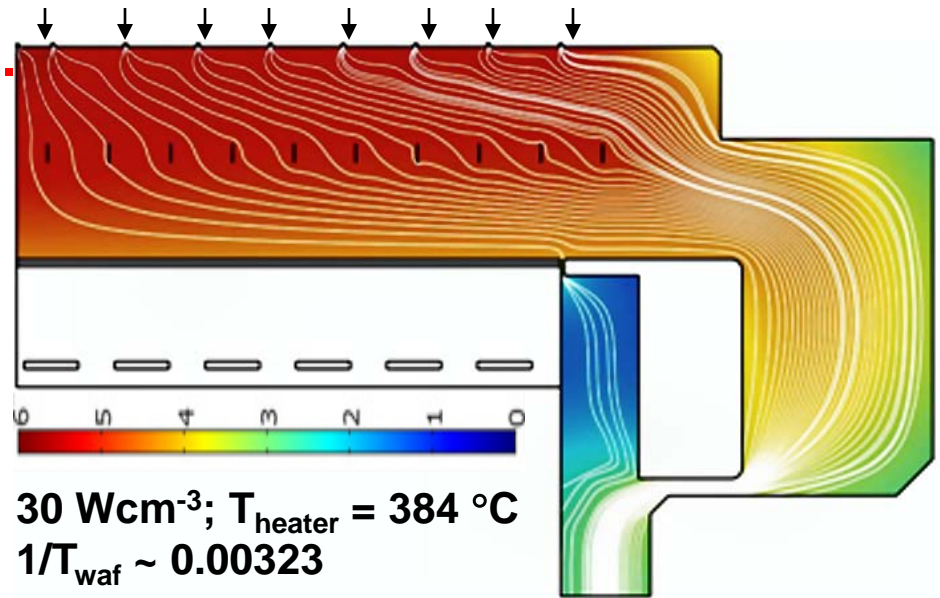
Ref.: J. Zhou, T.R. Ohno, and C.A. Wolden: The high temperature stability of nichrome in reactive environments. J. Vac. Sci. Technol. A 21(3), May/June 2003, 756-761



iCVD process development for SAC film



Simulation was performed at process conditions and iterating for sticking coefficient to fit deposition rate

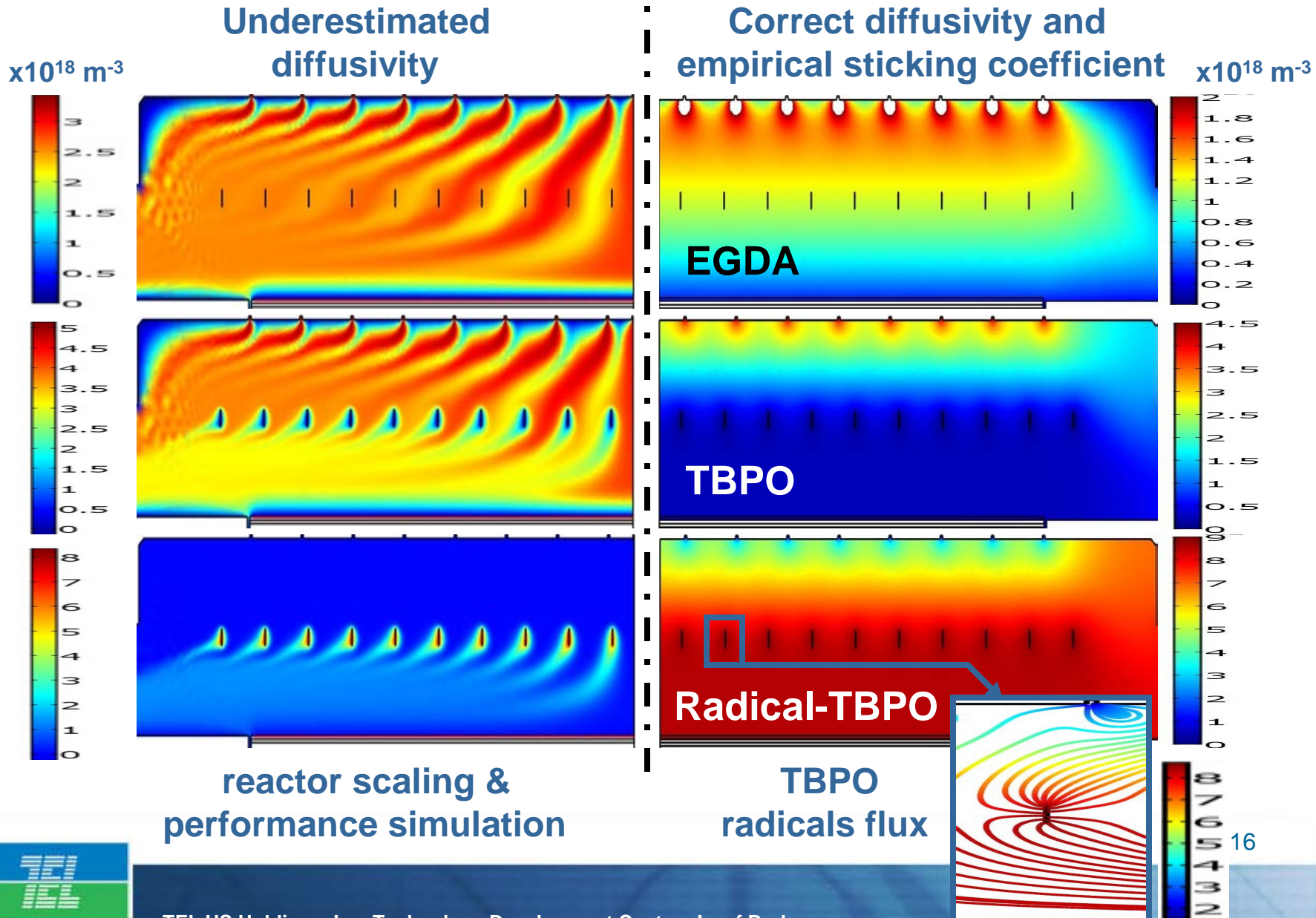


EGDA flux ~ 2x10¹⁵ molecules.cm⁻².s⁻¹

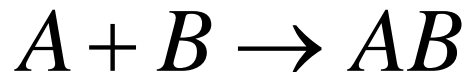
$$\zeta_{EGDA} \approx 0.023 \exp(0.5945/T)$$

S.H. Baxamusa, K.K. Gleason, *Initiated Chemical Vapor Deposition of Polymer Films on Nonplanar Substrates*, Proc. 5th Int. Conf. on HWCVD, MIT, Cambridge (2008)

Precursor transport

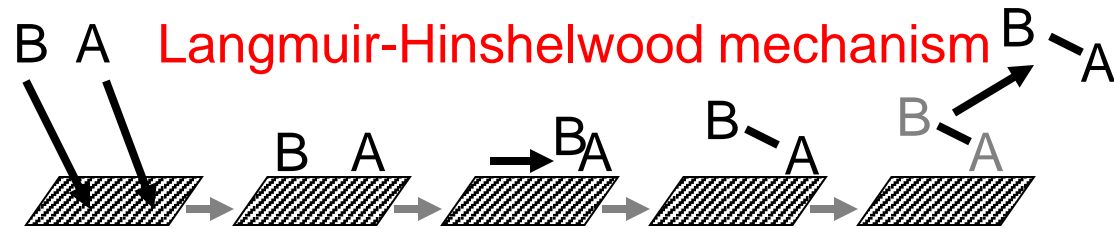


General mechanisms of surface reactions



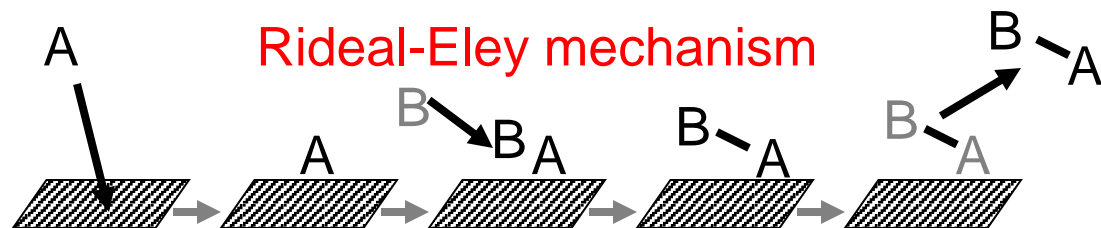
Langmuir-Hinshelwood mechanism

A and B first adsorb on the surface. Next, the adsorbed A and B react to form an adsorbed AB complex. Finally, the AB complex desorbs.



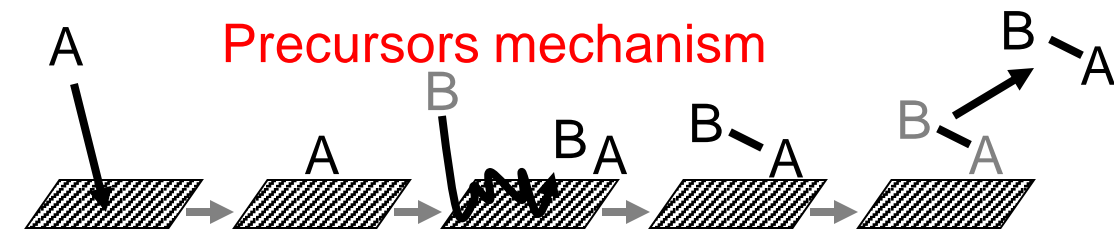
Rideal-Eley mechanism^[2]

The reactant A chemisorbs. The A then reacts with an incoming B molecule to form an AB complex. The AB complex then desorbs.



Precursors mechanism

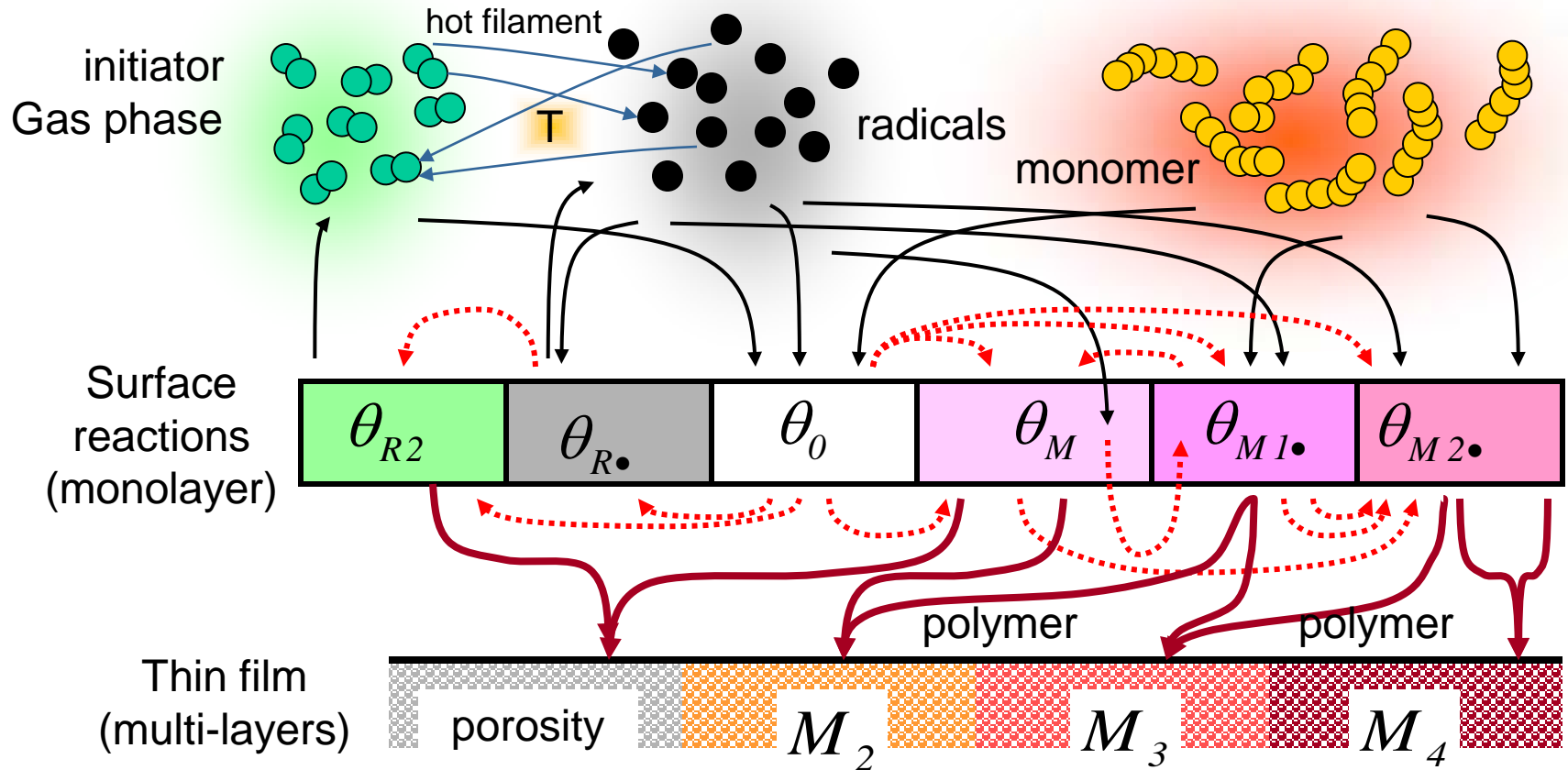
The reactant A adsorbs. Next, B collides with the surface and enters a mobile precursor state. The precursor rebounds along the surface until it encounters an adsorbed A molecule. The precursor then reacts with the A to form an AB complex, which desorbs.



[2] originally Rideal and Eley did not distinguish "precursor" mechanism within their definition of mechanism, however, more workers now make a distinction.

[1] Richard I. Masel, Principles of adsorption and reaction on solid surfaces. John Wiley & Sons, New York (1996) 444.

Mass transport and surface mechanism flow



- System can be analytically solved to compute surface fraction coverage and analyze polymer growth

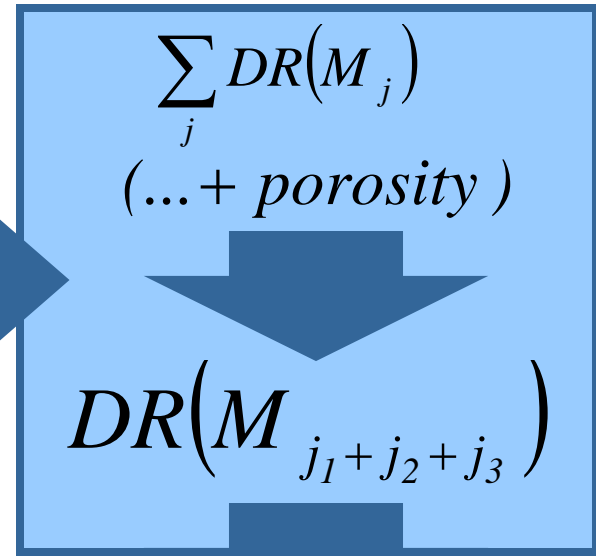
$$\theta_0^{solved}, \theta_{R2}^{solved}, \theta_{R\bullet}^{solved}, \theta_M^{solved}, \theta_{M1\bullet}^{solved}, \theta_{M2\bullet}^{solved}$$

Deposition rate and polymer composition

$$DR(M_2) = \left[\left(k_t^{a1} \theta_{M1}^2 + k_t^{b2} \theta_{M1} \theta_{M2} + k_t^{b3} \theta_{M2}^2 \right) \sigma_s^2 + k_t^{c2} \theta_{M2} n_R \sigma_s \right] V_{M2}$$

$$DR(M_3) = k_t^{a2} \theta_{M1} \theta_{M2} \sigma_s^2 V_{M3}$$

$$DR(M_4) = k_t^{a3} \theta_{M2}^2 \sigma_s^2 V_{M4}$$



Full surface chemistry models result in transcendent nonlinear equations - very complex solutions or unsolved cases

To avoid disambiguation within Comsol-based environment – substantially simplified versions of surface chemistry and solved analytically

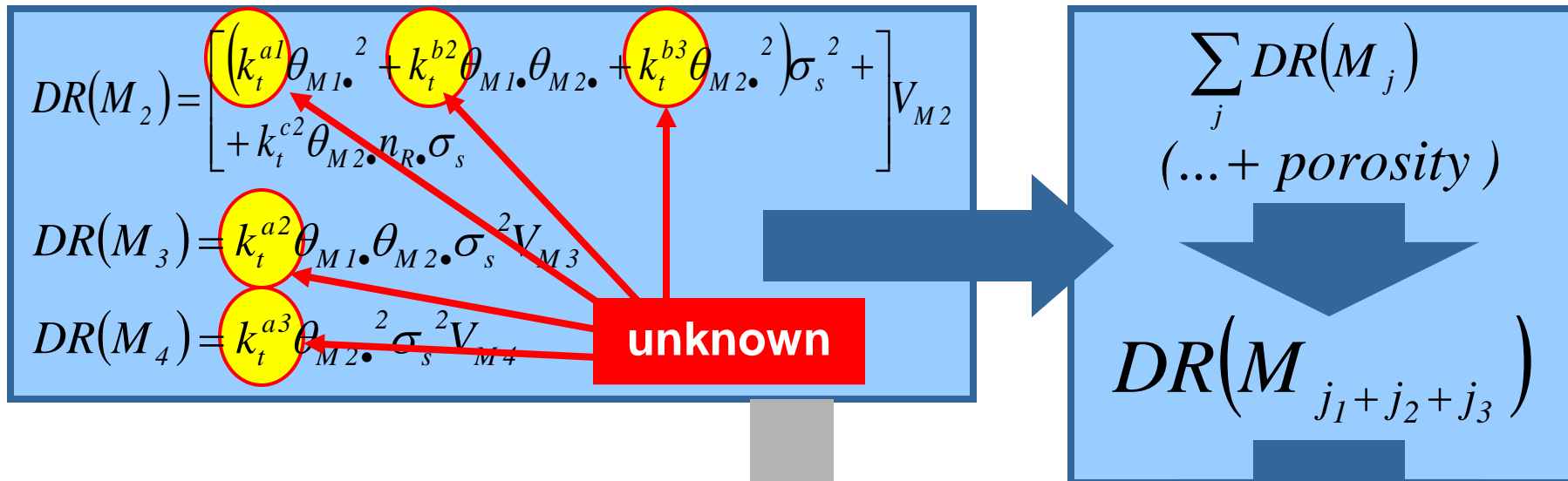
Advantage – fast computation

- ❑ **model designated to verify various hypothesis on film growth mechanism and determine empirical rate constants vs input parameters – process engineering & development**

Final film & structure of grown polymer is affected by many factors – post processing



Deposition rate and polymer composition



Methods used in Modeling & Simulation in Materials Science & Engineering

Final film & structure of grown polymer is affected by many factors – post processing

- model designated to verify various hypothesis on film growth mechanism and determine empirical rate constants vs input parameters – process engineering & development



Conclusions

❑ **Developed a pivotal model for FACVD / iCVD reactor. Baseline for investigation and virtual process development**

❑ **PROS / advantages**

- ✓ thermal performance was validated and it is in good agreement with experiments
- ✓ Determined sticking coefficient of EGDA monomer ~ 0.023 and effective activation energy ~ 4.94 J/mol for EGDA “iCVD mode polymerization”
- ✓ In virtual reactor, the film properties and complex processes can be adjusted simply by input parameters - computational DOE and hypothesis verification

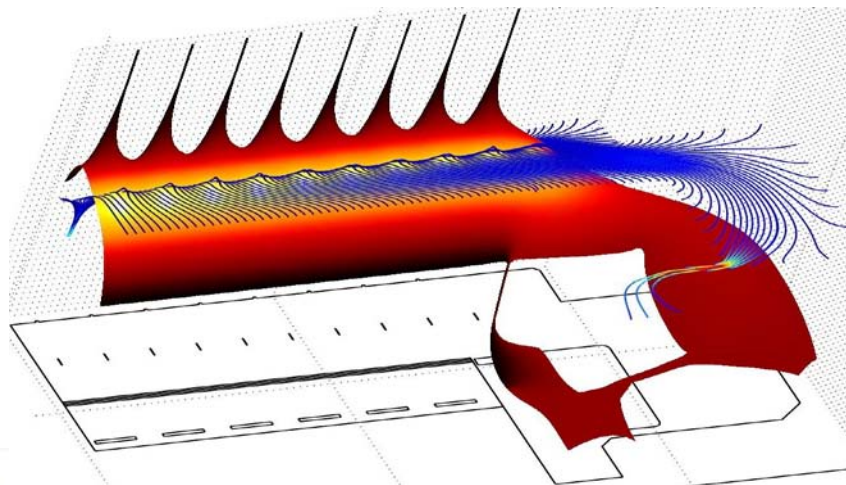
❑ **CONS / limitations**

- ✓ Too many adjusted and unknown parameters
- ✓ Surface chemistry to be enhanced – it relies on a growing experimental database



Acknowledgement

to Jacques Faguet, Eric Lee, Dorel Toma and Akiyama Osayuki for technological and application insights on FACVD / iCVD processes and experimental data.



□ Continuing work on upgrading chemistry, enhancing film growth model, conversion to pulsed operation, ...